STEM CELLS TRANSLATIONAL MEDICINE®

TISSUE-SPECIFIC PROGENITOR AND STEM CELLS

Expansion and Hepatic Differentiation of Adult Blood-Derived CD34$^+$ Progenitor Cells and Promotion of Liver Regeneration After Acute Injury

MIN HU,[a,*] SHAOWEI LI,[a,*] SIDDHARTH MENON,[a] BO LIU,[b] MICHAEL S. HU,[a,c,d] MICHAEL T. LONGAKER,[a,c] H. PETER LORENZ[a]

Key Words. CD34$^+$ • Cellular therapy • Hepatocyte differentiation • Liver regeneration • Hematopoietic progenitors • Adult stem cells

[a]Division of Plastic Surgery, Department of Surgery, [b]Division of Pediatric Surgery, Department of Surgery, and [c]Institute for Stem Cell Biology and Regenerative Medicine, School of Medicine, Stanford University, Stanford, California, USA; [d]Department of Surgery, John A. Burns School of Medicine, University of Hawaii, Honolulu, Hawaii, USA

*Contributed equally.

Correspondence: H. Peter Lorenz, M.D., Division of Plastic Surgery, Department of Surgery, School of Medicine, Stanford University, 257 Campus Drive, Palo Alto, California 94305, USA. Telephone: 650-736-1703; E-Mail: plorenz@stanford.edu

Received September 28, 2015; accepted for publication January 13, 2016; published Online First on April 13, 2016.

1066-5099/2016/$20.00/0

http://dx.doi.org/10.5966/sctm.2015-0268

ABSTRACT

The low availability of functional hepatocytes has been an unmet demand for basic scientific research, new drug development, and cell-based clinical applications for decades. Because of the inability to expand hepatocytes in vitro, alternative sources of hepatocytes are a focus of liver regenerative medicine. We report a new group of blood-derived CD34$^+$ progenitor cells (BDPCs) that have the ability to expand and differentiate into functional hepatocyte-like cells and promote liver regeneration. BDPCs were obtained from the peripheral blood of an adult mouse with expression of surface markers CD34, CD45, Sca-1, c-kit, and Thy1.1. BDPCs can proliferate in vitro and differentiate into hepatocyte-like cells expressing hepatocyte markers, including CK8, CK18, CK19, α-fetoprotein, integrin-β1, and A6. The differentiated BDPCs (dBDPCs) also display liver-specific functional activities, such as glycogen storage, urea production, and albumin secretion. dBDPCs have cytochrome P450 activity and express specific hepatic transcription factors, such as hepatic nuclear factor 1α. To demonstrate liver regenerative activity, dBDPCs were injected into mice with severe acute liver damage caused by a high-dose injection of carbon tetrachloride (CCl_4). dBDPC treatment rescued the mice from severe acute liver injury, increased survival, and induced liver regeneration. Because of their ease of access and application through peripheral blood and their capability of rapid expansion and hepatic differentiation, BDPCs have great potential as a cell-based therapy for liver disease. STEM CELLS TRANSLATIONAL MEDICINE *2016;5:723–732*

SIGNIFICANCE

Hematopoietic stem/progenitor cell expansion and tissue-specific differentiation in vitro are challenges in regenerative medicine, although stem cell therapy has raised hope for the treatment of liver diseases by overcoming the scarcity of hepatocytes. This study identified and characterized a group of blood-derived progenitor cells (BDPCs) from the peripheral blood of an adult mouse. The CD34$^+$ progenitor-dominant BDPCs were rapidly expanded and hepatically differentiated into functional hepatocyte-like cells with our established coculture system. BDPC treatment increased animal survival and produced full regeneration in a severe liver injury mouse model caused by CCl_4. BDPCs could have potential for liver cell therapies.

INTRODUCTION

Liver diseases affect hundreds of millions of people worldwide, and the incidence of acute or chronic liver failure has been increasing because of hepatitis viral infection, drug usage, alcohol abuse, and liver cancer [1, 2]. Hepatocyte transplantation by infusion of nonautologous cells is a promising method to promote liver regeneration for severe liver diseases [3, 4]. Despite some encouraging results, broader clinical applications have been hampered by the inability to expand adult hepatocytes in vitro [4, 5]. Stem cell technology has provided hope to identify new expandable sources of cells that can induce liver regeneration [6–8]. Adult stem cells that naturally exist outside the liver include mesenchymal stem cells (MSCs) and hematopoietic stem cells (HSCs) [9, 10]. CD34-expressing cells are normally considered to be primitive hematopoietic stem cells in embryonic tissues, adult bone marrow, umbilical cord blood, and human adult peripheral blood [11–13]. In recent years, many therapeutic applications with freshly isolated CD34$^+$ cells have been used in preclinical and clinical trials and have proved to be safe and effective in the treatment of liver diseases [14–16]. Although CD34$^+$ cells have

been reported to differentiate into all hepatic cell types in humans and animals, attempts to improve the engraftment potential of $CD34^+$ stem/progenitor cells have been largely unsuccessful owing to the inability to generate sufficient cell numbers [16, 17]. Furthermore, experience from in vitro studies indicates that control of their hepatic differentiation remains a challenge [18, 19].

We recently reported a coculture system that produces a group of $CD34^-$ MSCs from adult mouse peripheral blood. Treatment with $CD34^-$ MSCs enhanced healing of critical-size bone defects in the mouse calvaria [20]. In the present study, with a similar coculture system, we generated a group of blood-derived $CD34^+$ progenitor cells (BDPCs) from the nucleated fraction of nonmobilized peripheral blood of adult mice. The generated BDPCs were induced to expand rapidly and to differentiate specifically into hepatocyte-like or hepatic progenitor-like cells and demonstrated an ability to significantly promote liver regeneration after transplantation into mice with acute toxic liver injury.

Materials and Methods

Animals and Reagents

All animal care and procedures were performed in accordance with the guidelines from the Stanford University Administrative Panel of Laboratory Animal Care (protocol identification no. 11048). The donor animals were FVB-Tg (CAG-luc-eGFP) L2G85Chco/J (L2G) male mice harvested at 8 weeks of age (The Jackson Laboratory, Sacramento, CA, http://www.jax.org). The luc-eGFP transgene is directed by the CAG promotor (human cytomegalovirus immediate early promoter enhancer with chicken β-actin/rabbit β-globin hybrid promoter) that expresses enhanced green fluorescent protein (eGFP). One-time peritoneal injections (1.2 ml/kg) of CCl_4 diluted 1:1 in olive oil were performed on 20 adult recipient wild-type FVB mice at 8 weeks of age. One day after CCl_4 administration, the experimental mice were randomly chosen to accept a one-time intravenous injection with 2.5×10^5 differentiated BDPCs (dBDPCs) suspended in 150 μl of saline through the retro-orbital sinus ($n = 10$). The control mice were treated with 150 μl of saline by the same route ($n = 10$). All the mice were sacrificed on day 7 after the dBDPC transplantation. Blood was collected for laboratory measurements. The mouse internal organs were harvested and fixed in 10% buffered formalin. Liver tissue samples were separated for snap freezing and paraffin embedding.

The following primary antibodies were used as listed in Table 1. Horseradish peroxidase (HRP)-conjugated goat anti-rabbit secondary antibody (Bio-Rad Laboratories, Hercules, CA, http://www.bio-rad.com). ABC and 3,3′-diaminobenzidine (DAB) kits were purchased from Vector Laboratories (Burlingame, CA, http://www.vectorlabs.com). The culture medium, α-minimal essential medium (α-MEM), was purchased from Invitrogen (Life Technologies, Grand Island, NY, http:/www/thermofisher.com). Unless specified, all other chemicals were purchased from Sigma-Aldrich (St. Louis, MO, http://www.sigmaaldrich.com).

BDPC Isolation, Purification, and Coculture

Donor mice were fully anesthetized in a chamber supplied with 3% isoflurane (Butler Schein Animal Health, Encinitas, CA), and then injected with 3 U of heparin diluted in 100 μl of saline. The blood was collected through the retro-orbital sinus from each mouse using a heparinized capillary tube. Red blood cells were depleted by adding lysis buffer (8.3 g/l NH_4Cl, 1 g/l $KHCO_3$, 3.7 g/l EDTA at 10:1) to whole blood in a 50-ml tube, as previously reported [20], followed by high-speed centrifugation at 3,000*g* for 10 minutes at 4°C. The pellet was resuspended in 3 ml of phosphate-buffered saline (PBS). To deplete platelets, the cell suspension was transferred to a tube containing a 1:4.4 dilution of Optiprep Density Gradient Medium with PBS to a density of 1.063. The nucleated cell suspension was collected and centrifuged at 350*g* for 15 minutes at 4°C. The pellet was resuspended in PBS for further fluorescence-activated cell sorting (FACS) analysis or resuspended in the culture medium (α-MEM with 20% fetal bovine serum [FBS], 1× antibiotic-antimycotic, 20 mg of gentamicin) for in vitro studies. AML12 hepatic cells (ATCC, Manassas, VA, http://www/atcc.org) were pretreated with 30 mg/l mitomycin C for 2 hours. The mitotically inactivated AML12 hepatocytes were then inoculated on six-well plates in Dulbecco's modified Eagle's medium with 10% FBS. Sixteen hours after inoculation, the AML12 cells had adhered to the bottom chamber of culture wells and were approximately 80% confluent. The nucleated cell suspension derived from 0.5 ml of blood was placed into the upper chamber of a Transwell (24-mm insert, 0.4-μm pore size; Corning, Corning, NY, http://www.corning.com). The culture medium was changed every other day.

Table 1. Antibodies

Name	Source	Working dilution
A6	Dr. Valentina M. Factor, NIH, Bethesda, MD	50
AFP	Cell Signaling Technology, Inc., Beverly, MA	200
Albumin	Bethyl Laboratories, Montgomery, TX	3,000
β-actin	Santa Cruz Biotechnology, Santa Cruz, CA	1,000
CD117 (c-kit)	Biolegend, San Diego, CA	100
CD34	BD Biosciences, San Jose, CA	100
CD41	Biolegend, San Diego, CA	100
CD45	BD Biosciences, San Jose, CA	100
CK8	Santa Cruz Biotechnology, Santa Cruz, CA	500
CK18	Abcam, Cambridge, MA	500
CK19	DAKO, Carpentaria, CA	200
Integrin β1 (CD29)	Santa Cruz Biotechnology, Santa Cruz, CA	100
DNA antibody	Millipore, Billerica, MA	100
Ki-67	Novus Biologicals, Littleton, CO	250
PCNA	Novocastra laboratories, Newcastle, U.K.	200
Sca-1	BD Biosciences, San Jose, CA	100
Thy1.1 (CD90.1)	Abcam, Cambridge, MA	100

Abbreviations: AFP, α-fetoprotein; PCNA, proliferating cell nuclear antigen.

Magnetic-Activated Cell Sorting and FACS Analysis of BDPCs

After 3 weeks of coculture with AML12 cells, the expanded cells were purified with magnetic-activated cell sorting (MACS) to

enrich for CD34-positive cells (Miltenyi Biotec Inc., San Diego, CA, http://www/miltenyibiotech.com). In brief, cultured cells were trypsinized and incubated with an anti-CD34 rat antibody for 30 minutes, washed with PBS, and incubated with anti-rat microbeads at 4°C for 30 minutes. After being washed with PBS, the cells were resuspended in 500 μl of separation buffer and applied onto a MACS column. Cells from the original, negative, and positive fractions were counted and seeded onto the Transwell membrane as mentioned above. The expanded cells were analyzed for CD34 positivity and different surface markers, including CD45, Sca-1, Thy1.1, c-kit, and CD41 by FACS. Nuclei were stained with 4′,6-diamidino-2-phenylindole (DAPI) or Hoechst 33342. Data were analyzed using FlowJo (Tree Star, Ashland, OR, http://www/flowjo.com).

Polymerase Chain Reaction, Reverse Transcription Polymerase Chain Reaction, and RNA Analysis

DNA was extracted from fresh or frozen liver tissues from cultured BDPCs, eGFP mice, or dBDPC-transplanted mouse livers using a GENJET Genomic DNA purification kit (ThermoScientific, Vilnius, Lithuania, http://www.thermofisher.com). Total RNA was extracted from MACS-sorted, Hoechst 33342-positive, fresh or cultured BDPCs at 3 weeks or control cells (cultured AML12 cells without any treatment) using the Trizol reagent method and then treated with RNase-free DNase to remove contaminated DNA. First-strand cDNA was obtained from 4 μg of total RNA per 100 μl of reaction volume using SuperScript II reverse transcriptase (Life Technologies, Carlsbad, CA). Polymerase chain reaction (PCR) and reverse transcription-PCR were performed in a 20-μl reaction volume with a standard protocol and 1,000 ng of template DNA or cDNA, 10 μM of each primer, and PCR Master Mix (Promega, Madison, WI, http://www.promega.com). Primers for PCRs were designed using Primer3 (Table 2). 18S rRNA was used as an internal control gene.

Western Blot Analysis

Cultured BDPCs and AML12 cells were washed three times with PBS and then lysed with RIPA buffer and incubated on ice for 15 minutes. The lysates were centrifuged, and the supernatant was used for Western blot analysis after protein quantification. Cell lysates were transferred to nitrocellulose membrane by electrophoresis. After washing, the protein-loaded membrane was incubated with dry milk to block nonspecific binding. The primary antibody incubation used a rabbit anti-albumin antibody and a β-actin antibody for internal quantity control, at 4°C, overnight. After washing, the membrane was incubated with HRP-conjugated goat anti-rabbit secondary antibody and visualized by enhanced chemiluminescence (GE Healthcare, Little Chalfont, Buckinghamshire, United Kingdom, http://www3.gehealthcare.co.uk).

Histological and Immunological Staining

Paraffin-embedded tissue specimens were sectioned at 5-μm thickness on glass slides and deparaffinized and rehydrated. Freshly isolated or cultured BDPCs and cultured AML12 cells were cytospun onto glass slides or directly tested on the Transwell membrane. The tissue or cell slides and Transwell membranes were stained with hematoxylin and eosin or periodic acid-Schiff (PAS). Immunohistochemistry (IHC) and immunofluorescence (IF) staining are briefly described as follows: the slides underwent antigen retrieval in 0.01 M citric acid buffer, pH 6.0, in a microwave oven for 5 minutes, followed by incubation with 0.03% H_2O_2 for 30 minutes to block endogenous peroxidase. The slides and membranes were incubated with 1% horse serum for 30 minutes to block nonspecific binding and then incubated with primary antibodies overnight at 4°C. After washing with PBS, the slides were treated with biotinylated secondary antibodies for IHC or fluorescent dye-conjugated antibodies for IF. Alexa Fluor anti-mouse, anti-rabbit, or anti-rat IgG1 antibodies (1 μg/ml) were used as antibody controls. IF-stained slides were mounted with DAPI and analyzed by confocal microscopy. IHC samples were incubated with ABC complex and then developed with DAB. Double staining was developed with DAB (brown stain) and nickel/DAB (dark blue or gray stain). Diverse control groups, including positive, negative, and blank controls, were set up for each test to ensure the specificity of the antibodies. The images were viewed under a Leica DMRA microscope (Leica, Heerbrugg, Switzerland, http://www.leica.com).

In Situ Imaging of GFP Expression in the Liver

Liver specimens were flushed with cold saline (4°C, 10 ml) and embedded into Cryo-OCT Compound (Sakura Finetek, Tokyo, Japan, http://www.sakura-finetek.com) directly without fixation to avoid the autofluorescence caused by aldehyde crosslinking. The fluorescence of the GFP signal in liver tissues was measured by fluorescence microscopy.

Statistical Analysis

Statistical analysis was performed using a paired, two-tailed Student's *t* test to compare two groups. Image analysis was performed with ImageJ (NIH, Bethesda, MD, http://www.imagej.nih.gov), a Java-based image processing program. Differences were considered significant when $p < .05$.

RESULTS

Isolation and Expansion of BDPCs

FACS analysis of freshly isolated nucleated cells from the peripheral blood of L2G or wild-type FVB mice demonstrated a highly heterogeneous cell mixture after red blood cell lysis and platelet depletion. A small fraction of CD34-positive cells coexpress CD45 (0.04% in two pooled mouse fractions; Fig. 1A). The nucleated ($DAPI^+$) cell mixture from peripheral blood of L2G (GFP^+) mice rapidly expanded during coculture with AML12 hepatocytes. Figure 1B illustrates the proliferation differences of the cells under coculture and without coculture on days 0, 5, and 15 ($p < .001$). However, the cell mixture without coculture with AML12 cells did not proliferate and became senescent, with loss of GFP expression by day 5 compared with the cocultured cells (Fig. 1B–1D). Although only a very few $CD34^+$ cells were found in the peripheral blood of the adult mice, the $CD34^+$ cell numbers increased 11-fold during coculture within 3 weeks.

Characterization of BDPCs

After being enriched by MACS, the $CD34^+$ cell dominant group (>90%) expanded more rapidly in the hepatic environment over time. FACS analysis demonstrated that the expanded BDPCs not only expressed CD34 but also expressed CD45 and c-kit (Fig. 2A–2C), not CD41, the molecular marker for blood platelets (Fig. 2D). Bromodeoxyuridine labeling showed that the

Table 2. Primers for PCRs

Gene	Forward primer	Reverse primer
18S	ACGGCTACCACATCCAAGGA	CAATTACAGGGCCTCGAAAGAG
Cyp 3A16	GATTCCCTCAACAACCCAGA	AATCCTTTGGGAACATGCAG
Cyp1B1	GAATCATGACCCAGCCAAGT	AGATTCTGGCAAGGCTTCAA
HNF1α	TGCCTGTTTGAGGATTACCC	ACATCCAAGGGAACAGATGG
eGFP	GCAAGCTGACCCTGAAGTTCATC	TCACCTTGATGCCGTTCTTCTG
Alb/Cre	TGCCACGACCAAGTGACAGCAATG	AGAGACGGAAATCCATCGCTCG
mTmG	CTCTGCTGCCTCCTGGCTTCT	CGAGGCGGATCACAAGCAATA
	mTmG reverse-mutant	TCACCTTGATGCCGTTCTTCTG

Abbreviations: Alb, albumin; eGFP, enhanced green fluorescent protein; HNF1α, hepatic nuclear factor 1α; PCR, polymerase chain reaction.

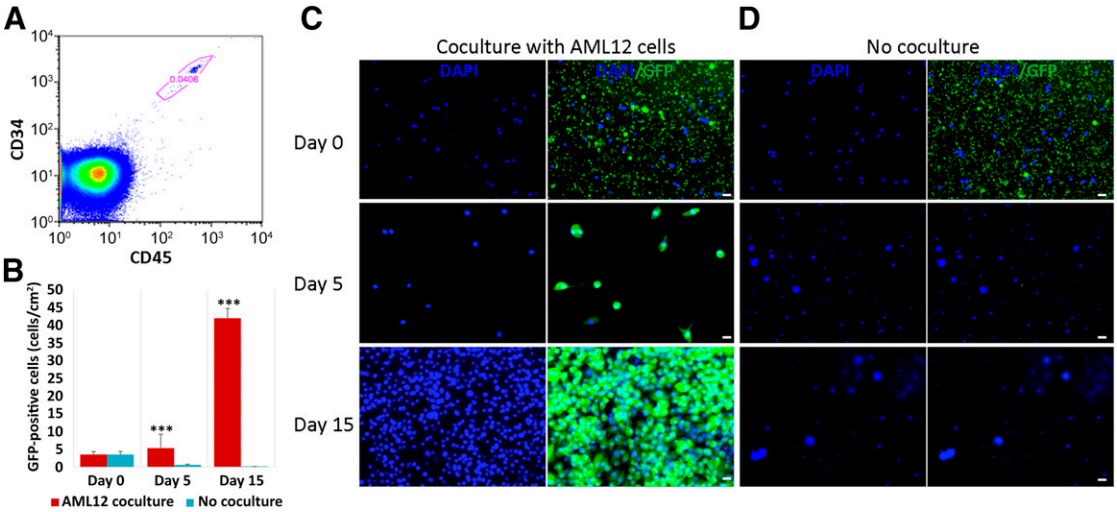

Figure 1. Isolation and expansion of blood-derived CD34+ progenitor cells. **(A):** Fluorescence-activated cell sorting analysis of the nucleated cell mixture after depletion of erythrocytes and platelets demonstrated that a small fraction of CD34-positive cells coexpresses CD45 (0.04%) from the pooled peripheral blood of two adult FVB-Tg (CAG-luc-eGFP) L2G85Chco/J L2G mice. **(B):** The proliferation difference of the nucleated mixture with and without AML12 cell coculture on days 0, 5, and 15 is quantitatively illustrated. ***, $p < .001$). **(C):** The nucleated (DAPI+) cell mixture from FVB-Tg (CAG-luc-eGFP) L2G85Chco/J L2G mouse blood (GFP positive) rapidly expanded during coculture with AML12 cells. **(D):** The cell mixture without coculture with AML12 cells did not proliferate and became senescent with loss of GFP expression by day 5. Scale bars = 5 μm. Abbreviations: DAPI, 4′,6-diamidino-2-phenylindole; GFP, green fluorescent protein.

CD34+-enriched BDPC doubling time was about 48 hours (Fig. 2E). Immunofluorescent double staining was performed to determine the association between CD34 and CD45 on BDPCs (Fig. 2F). BDPCs also express Sca-1 (Fig. 2G) and Thy1.1 (CD90.1; Fig. 2H).

Hepatic Differentiation of BDPCs

Pronounced morphological changes in expanded BDPCs during AML12 coculture over time were observed. The BDPCs become elongated, flat, and polygonal, with a decreased ratio of nucleus to cytoplasm after 4 weeks of coculture. The cocultured BDPCs expressed a diverse panel of markers for hepatocytes such as α-fetoprotein (AFP), CK8, CK19, and CK18 (Fig. 3A, 3B, 3D, 3E). A6, a specific marker for intrahepatic stem cells, was coexpressed with proliferating cell nuclear antigen (PCNA) and CK19 (Fig. 3C, 3D). Coexpression of hepatic epithelial markers CK8 or CK18 and CD34 in the same BDPCs suggested hepatic epithelial differentiation is occurring. Some BDPCs demonstrated colocalization of PCNA with A6, suggesting active proliferation of primitive hepatocyte-like cells. CD45 positivity on BDPCs growing in situ on the Transwell membrane demonstrated their hematopoietic origin (Fig. 3F). Hepatic-specific transcription factors and liver metabolic function-related cytochrome P450 (CYPs) genes, such as hepatic nuclear factor 1α (*HNF1α*), *CYP3A16*, and *CYP1B1*, were activated in BDPCs compared with AML12 hepatocytes (Fig. 3G).

In order to study the mechanism of BDPC transdifferentiation, mT/mG mice (The Jackson Laboratory, Bar Harbor, ME, http://www.jax.org) were crossed with albumin-Cre transgenic mice (courtesy of Dr. Karl Sylvester, Stanford, CA). The transdifferentiation process of BDPCs from hematopoietic cells to hepatic-epithelialized, albumin-expressing cells under the induction of the hepatic environment was observed. Freshly isolated nucleated cells from mT/mG mice all expressed the Tomato red transgene, as expected. During coculture with AML12 cells, some BDPCs converted to green fluorescence as albumin/Cre transgene was expressed by day 7. Most cells gradually turned green and expressed GFP over time (Fig. 4A–4C). CD29, an important regulator of liver functional differentiation, was expressed in the GFP+ BDPCs (Fig. 4D). Positive PAS staining suggested functional activity of the dBDPCs to synthesize and store glycogen (Fig. 4E), in addition to albumin expression (Fig. 4F). The growth

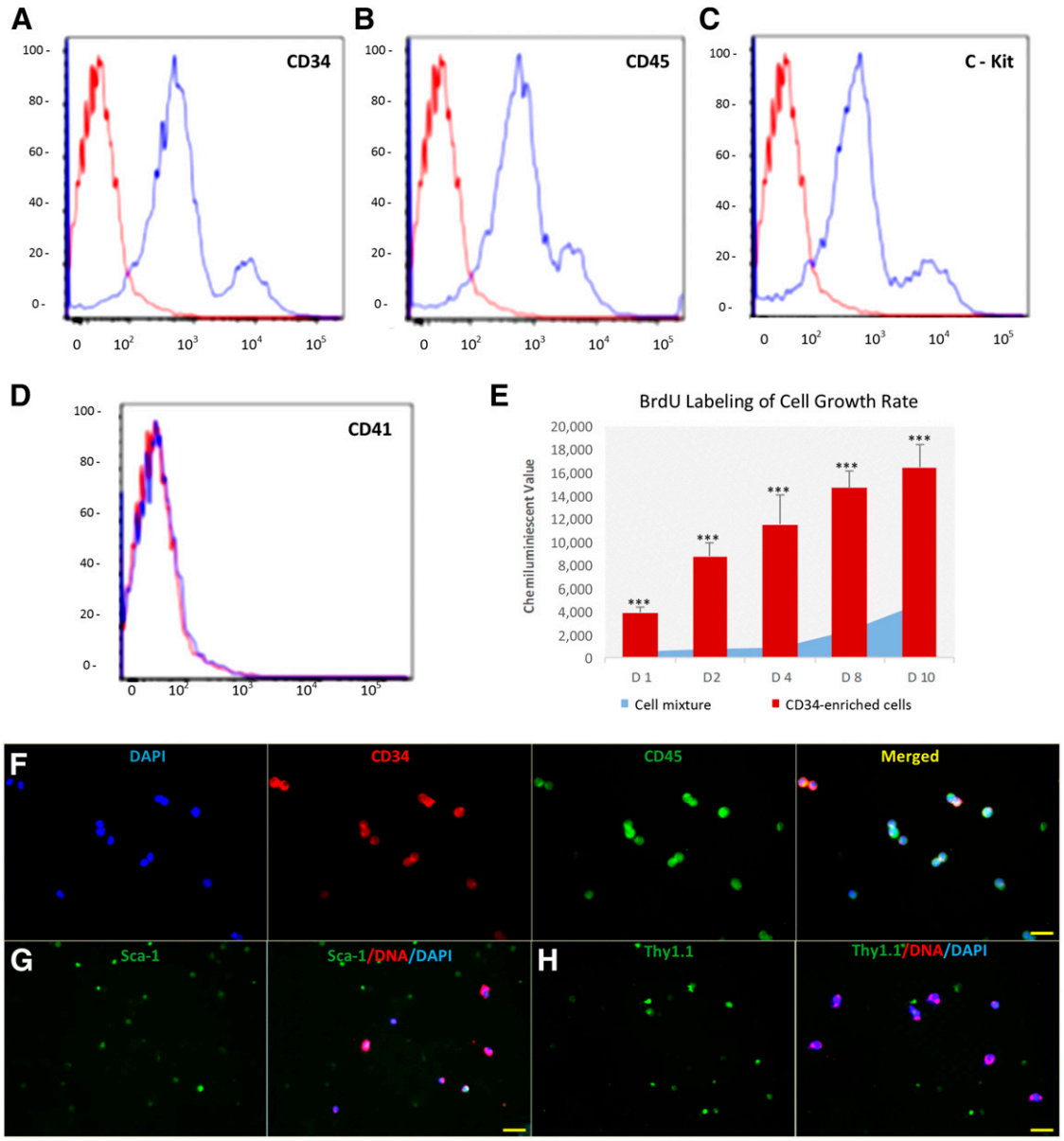

Figure 2. Characterization of expanded blood-derived $CD34^+$ progenitor cells (BDPCs). **(A–D):** Fluorescence-activated cell sorting analysis of expanded BDPCs demonstrates the expression of CD34, CD45, and c-kit but no expression of the platelet marker CD41. **(E):** CD34-enriched BDPCs proliferated with a doubling time of approximately 48 hours during coculture (***, $p < .001$). **(F):** Immunofluorescent double staining confirmed coexpression of surface markers CD34 and CD45 on BDPCs. **(G, H):** BDPCs also expressed stem cell markers Sca-1 and Thy1.1 (CD90.1). Scale bars = 5 μm. Abbreviations: BrdU, bromodeoxyuridine; DAPI, 4′,6-diamidino-2-phenylindole.

status of the differentiated BDPCs was explored with Ki-67, a cell proliferation marker. Some dBDPCs showed proliferative activity (Ki-67, red fluorescence) with albumin expression (green fluorescence; Fig. 4G). Immunoblotting demonstrated increased albumin expression over time in cocultured dBDPCs (Fig. 4H).

dBDPCs Promote Liver Regeneration

An acute liver injury mouse model was successfully created by high-dose CCl_4 injection. Starting at day 1 after injection of CCl_4, each mouse lost 1–2 g of body weight (BW) daily. The BW of the mice without dBDPC treatment (saline treated as control) continued to decrease until the mice were sacrificed on day 7, consistent with worsening liver damage (Fig. 5A). Two mice (20% mortality) died on days 2 and 3 after CCl_4 injection. Saline-treated mice also had a higher ratio of liver weight to BW due to inflammatory hepatomegaly, characteristic of acute liver injury (Fig. 5B). In contrast, all mice treated with dBDPCs survived and showed a remarkable recovery pattern: the BW decreased for 1 or 2 days, followed by stability or an increase in BW to baseline. The lost BW had been regained by all dBDPC-treated mice by day 5 after CCl_4 injection (or day 4 after dBDPC treatment).

A dramatic increase in serum alanine transaminase (ALT) levels of all mice to greater than 350 times normal at 1 day after CCl_4 administration was observed (Fig. 5C), indicating severe liver cell damage. On the day of sacrifice (day 7), the aspartate

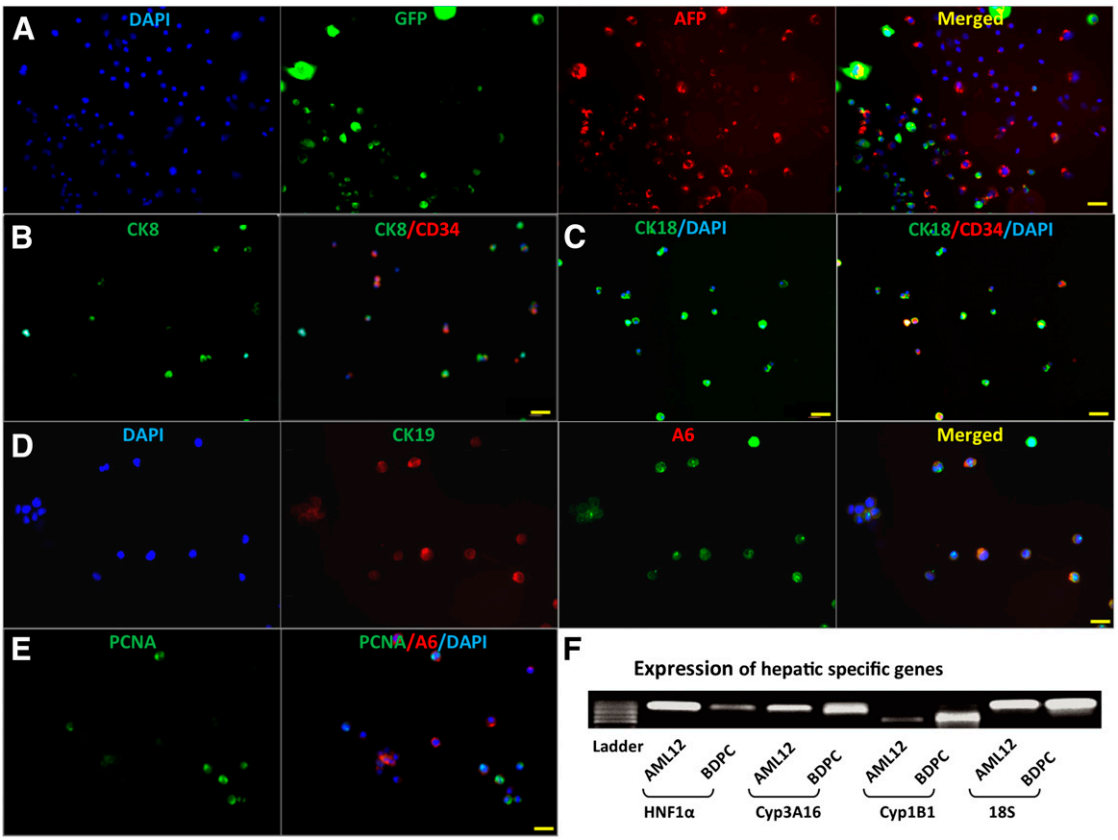

Figure 3. Blood-derived CD34+ progenitor cells (BDPCs) express hepatocyte and hepatic progenitor markers in vitro. **(A):** Cultured GFP-positive BDPCs expressed AFP. **(B, C):** Coexpression of hepatic epithelial marker CK8, CK18, and CD34. **(D):** Coexpression of CK19 and A6. **(E):** Coexpression of PCNA and A6. **(F):** Expression of hepatic-specific transcription factor and liver metabolic genes, cytochrome P450 subgenes in cocultured BDPCs compared with AML12 hepatocytes. Scale bar = 10 μm. Abbreviations: AFP, α-fetoprotein; DAPI, 4′,6-diamidino-2-phenylindole; GFP, green fluorescent protein; PCNA, proliferative cell nuclear antigen.

transaminase (AST) level, ratio of AST/ALT, and urea level were significantly higher in the saline-treated mice compared with dBDPC-treated mice (Fig. 5D, 5E).

Consistently, histological analysis showed centrilobular necrosis characteristic of CCl_4 hepatic toxicity in saline-treated mouse livers. Hepatocytes in the centrilobular region demonstrated vacuolar, hydropic, and fatty degeneration accompanied by pyknosis, karyorrhexis, and karyolysis in saline-treated mouse livers on day 7 (Fig. 5H) compared with normal livers (Fig. 5G, 5H). In contrast, dBDPC-treated mice demonstrated complete regeneration with near normal structure in the central vein area. These findings suggest dBDPC treatment markedly attenuates CCl_4 damage and greatly promotes liver regeneration. Of note, the inflammatory cells did not infiltrate the regenerated liver area and surrounding tissues after dBDPC treatment, suggesting little rejection or immune response occurs (Fig. 5I). Analysis of the regional necrosis demonstrated a significant difference in dBDPC-treated mice based on the necrotic cell count between the dBDPC-treated and saline-treated mouse livers ($p < .001$; Fig. 5F). Fluorescent microscopy demonstrated considerable numbers of GFP+ cells in the central vein region, which is the target of CCl_4 injury. The GFP+ cells engrafted in the damaged area (Fig. 5J).

After dBDPC treatment to the acute liver injury model, GFP-positive dBDPCs were present in the regenerating hepatic central vein regions. Transplanted GFP+ cells (Fig. 5K, brown color) expressed albumin (Fig. 5K, arrowhead, dark gray) and the proliferation marker Ki-67 (Figure 5L, arrowhead, blue). These findings suggest that the transplanted dBDPCs are accepted by the host liver and are not transient, but actively proliferate and repopulate the damaged region both structurally and functionally. PCR analysis of the liver tissue showed the long-term presence of the GFP gene in the transplanted liver for at least 3 months (Fig. 5G). We found no gross or histologic evidence of hepatic tumor formation in the dBDPC-treated livers at all time points.

Discussion

HSC expansion and tissue-specific differentiation in vitro are considered challenges in regenerative medicine [21, 22]. In the present study, we report that a group of CD34+ cells, derived from the peripheral blood of adult mice, can be induced to expand rapidly and further undergo hepatic differentiation into functional hepatic cells while obtaining the ability to promote liver regeneration.

Many recent clinical and experimental efforts have tried to enhance HSC expansion and differentiation in vitro with growth factors or cytokines, with the rationale to mimic stimulations to HSC/progenitor cells from their bone marrow microenvironmental niches [23–25]. The liver is the primary site of hematopoiesis during mammalian prenatal development, and hepatic hematopoiesis is believed to persist into adulthood [14, 26, 27]. Based on the hypothesis

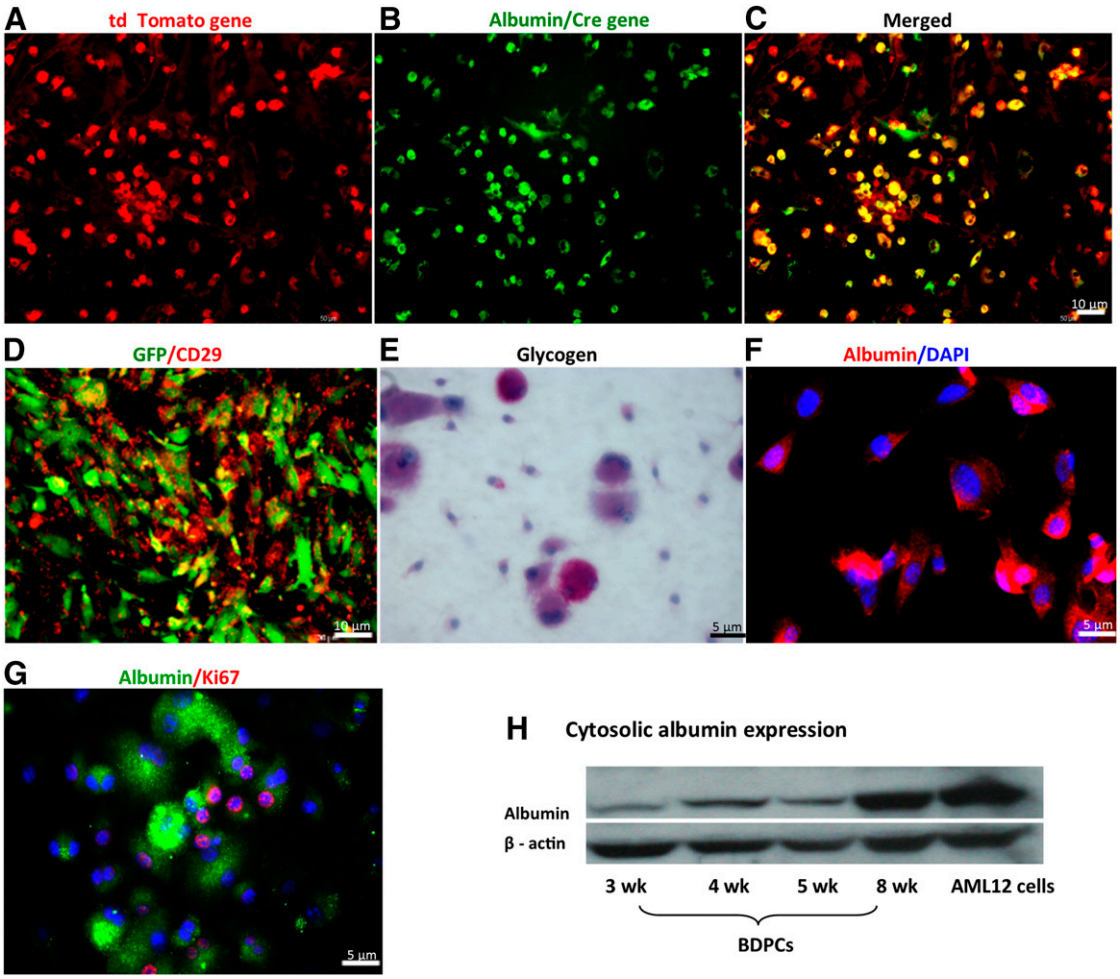

Figure 4. Transdifferentiated BDPCs demonstrate hepatocyte-like function. **(A–C):** BDPCs isolated from mT/mG mouse gradually became green as their albumin/Cre transgene was expressed over time in coculture with AML12 cells. **(D):** Immunofluorescent staining demonstrated expression of integrin β (CD29) in GFP$^+$ BDPCs. **(E):** Periodic acid-Schiff staining showed that glycogen was synthesized and stored in BDPCs in situ on the Transwell membrane. **(F):** BDPCs expressed albumin protein. **(G):** Coexpression of albumin and Ki-67 indicated proliferation of some transdifferentiated BDPCs in vitro in coculture. **(H):** Immunoblot shows that cytosolic albumin protein levels in BDPCs increased during extended culture. Scale bars = 10 μm **(A–D)** and 5 μm **(E–G)**. Abbreviations: BDPCs, blood-derived CD34$^+$ progenitor cells; DAPI, 4′,6-diamidino-2-phenylindole; GFP, green fluorescent protein.

that the liver environment might be beneficial to HSC proliferation and hepatic differentiation, we successfully induced CD34$^+$ cells to expand, differentiate, and promote hepatic regeneration after acute injury.

CD34$^+$ cells are 0.04% of the nucleated cell population in the circulating peripheral blood of two adult mice. This low amount of CD34$^+$ cells necessitates expansion to develop their use as a cell-based therapy. Our coculture protocol for expansion of CD34$^+$ cells uses a two-step strategy. First, coculture is initiated with the total nucleated cell fraction. The next step is to enrich for CD34$^+$ cells by MACS and then continue the coculture with a more purified CD34$^+$ cell population. As a result, CD34$^+$ BDPCs in the nucleated cell fraction are rapidly expanded 11-fold within 3 weeks. The dBDPC culture system started with a highly heterogeneous cell mixture, including residual platelets and/or cellular debris. However, anucleated cells and debris were washed out with changes of media. We confirmed the absence of platelets by demonstrating a lack of CD41 expression, a platelet marker, in cultured dBDPCs.

FACS analysis confirmed the purity of the collected CD34$^+$ cells as $>$90% in the cell population after MACS enrichment. CD34$^+$ dBDPCs are highly proliferative with a doubling time of 48 hours. dBDPCs can be expanded robustly in vitro to achieve a quantity sufficient for further transplantation in vivo. dBDPCs have been passaged for more than 64 generations and maintained for over 2 years. Expression of CD34 remains on the cells over time.

Previous studies have shown that the hepatic program can be activated in nonhepatic lineage cells after exposure to particular stimuli [21, 22]. Soto-Gutiérrez et al. induced mouse embryonic stem cells to differentiate into hepatocyte-like cells by coculture with human liver nonparenchymal cells [28]. Alaimo et al. successfully induced peripheral blood-derived stem cells into hepatocyte-like cells by coculture with freshly isolated hepatocytes [29]. However, hepatocyte collection is a time-consuming process, and freshly isolated hepatocytes are unable to remain functional and maintain hepatic characteristics in culture. Recently, Mu et al. induced human adult multipotent progenitors into hepatocyte-like cells by coculture with the human hepatocyte line L02 [30]. These studies all reported that the hepatic environment is beneficial for hepatic differentiation of stem cells. The AML12 cell line was established from hepatocytes from a CD1 strain transgenic mouse. AML12 cells exhibit typical

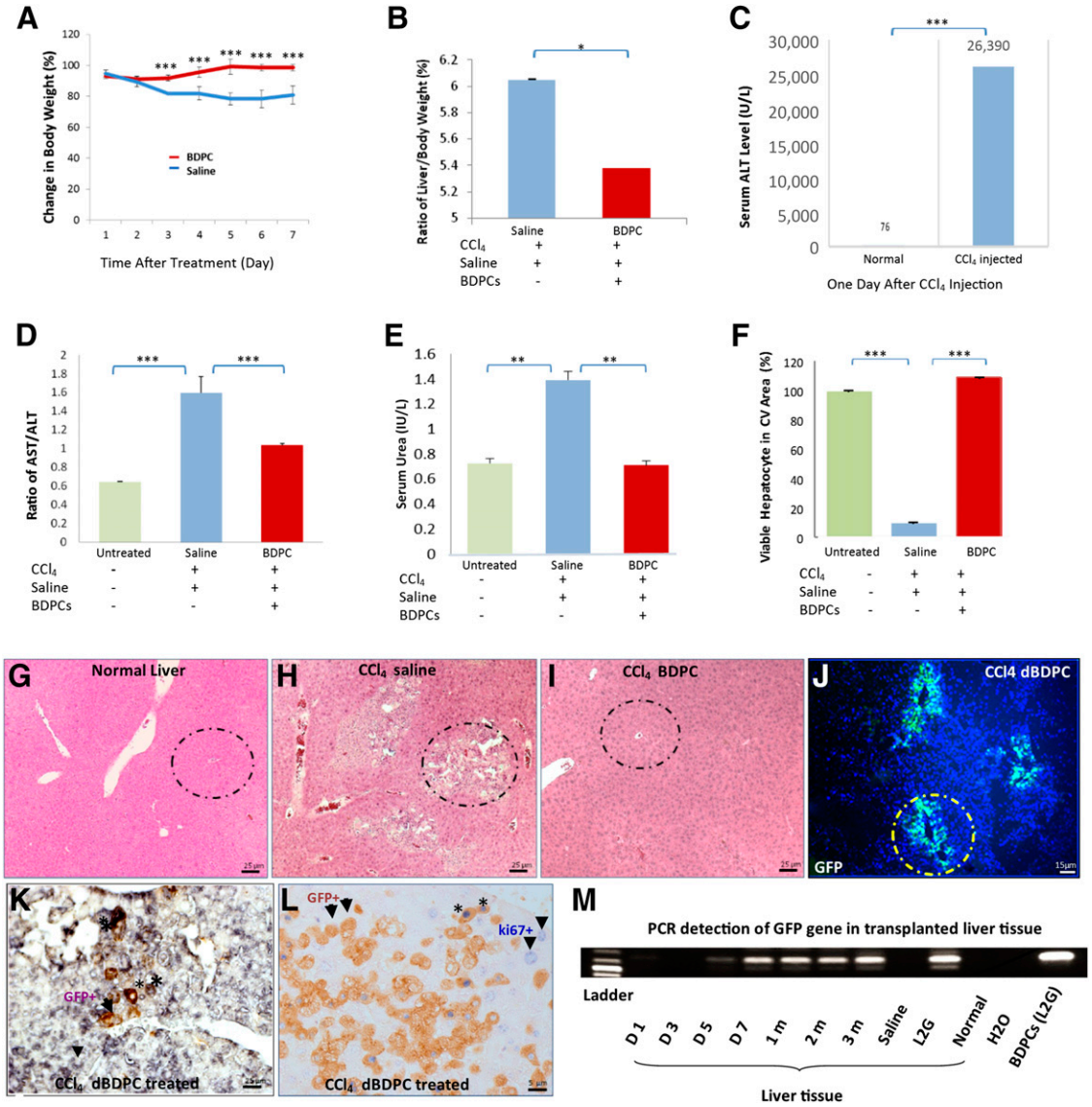

Figure 5. dBDPC treatment promotes liver regeneration after acute injury. **(A):** Changes in body weight of CCL_4-injected mice show that dBDPC treatment (red line) restored body weight after CCL_4 injury. **(B):** The ratio of liver weight to body weight of the saline-treated mice was higher than that of the dBDPC-treated mice, indicating hepatomegaly of saline-treated mice. **(C):** Serum ALT level sharply increased more than 300 times normal in all mice 1 day after CCL_4 injection. **(D):** On the day of sacrifice, the AST/ALT ratio in the dBDPC-treated mice had a significantly lower value than that of control saline-treated mice. **(E):** Urea levels showed nearly fully recovered hepatic metabolic function in mice treated with BDPCs. **(F):** Regional hepatic necrosis was decreased in dBDPC-treated compared with saline-treated mouse livers. *, $p < .5$; **, $p < .05$; ***, $p < .001$. **(G):** The dashed circle shows a central vein area in a normal (no injury) mouse liver (H&E stain). **(H):** Saline-treated mouse liver after CCl_4 injury demonstrated typical centrilobular necrosis on day 7 (H&E stain). **(I):** Mouse liver after dBDPC treatment (day 7) manifested full structural regeneration (H&E stain). **(J):** GFP-positive cells present in the damaged centrilobular region in mouse liver after dBDPC treatment (fluorescent channel). **(K, L):** Double-color immunohistochemical staining showed that GFP^+ dBDPCs (brown or orange) coexpressed albumin (arrowheads, dark gray) or Ki-67 (arrowheads, blue), a cell proliferative marker, in the injured liver tissue. **(M):** PCR analysis of the liver tissue revealed long-term presence of GFP from day 5 to 3 months after dBDPC treatment. Scale bars = 25 μm **(G–K)**, 15 μm **(J)**, and 5 μm **(L)**. Abbreviations: ALT, alanine transaminase; AST, aspartate transaminase; BDPC, blood-derived $CD34^+$ progenitor cells; CV, central vein; dBDPC, differentiated BDPC; GFP, green fluorescent protein; PCR, polymerase chain reaction.

hepatocyte features and express high levels of specific hepatic proteins, such as albumin, yet they are not transformed cells [31]. Therefore, in the present study, the AML12 cell line was chosen as the feeder cell to create a hepatic environment for the differentiation of BDPCs. Our pilot experiments with AML12-conditioned medium yielded similar hepatic differentiation of BDPCs (data not shown). The specific proteins present in the conditioned medium responsible for hepatic BDPC differentiation are under current investigation.

Intrahepatic progenitor stem cells, named oval cells, are located in the canals of Hering in the liver. Oval cells express CK18, CK19, AFP, albumin, and A6 and are reported to differentiate into hepatic functional cells during liver regeneration after severe liver injury [32–34]. We found that BDPCs cocultured with AML12 hepatic cells differentiate into hepatocyte-like and hepatic progenitor-like cells with expression of the same markers as oval cells.

The expression of liver metabolic enzymes, such as the CYP genes, demonstrated fully mature hepatocyte function. dBDPC-derived hepatocyte-like cells showed activated gene expression of CYP3A16 and CYP1B1 and a liver-associated specific transcription factor (HNF1α). Thus, BDPCs were induced toward hepatic differentiation in coculture.

Stem cell plasticity or transdifferentiation describes the process of an adult stem cell acquiring the phenotype of a mature cell distinct from its tissue of origin [35, 36]. The mT/mG mouse is a double-fluorescent Cre reporter transgenic mouse that expresses a membrane-targeted tandem dimer Tomato (mT) before Cre-mediated excision and membrane-targeted green fluorescent protein (mG) after excision. The mT/mG mouse system has been used to study conditional gene alterations [37, 38]. The prediction for the crossed mT/mG and albumin/Cre mouse was that all cells from the mT/mG mouse are engineered to constitutively express a conditional red fluorescent transgene that converts to GFP expression after exposure to albumin/Cre recombinase. Our results have shown that all cells in the nucleated cell fraction of peripheral blood of adult mT/mG mice express the red fluorescent transgene after isolation. However, during coculture with AML-12 cells, BDPCs express GFP as they begin to express albumin. This result, together with coexpression of hepatic epithelial markers, hepatic stem cell markers, hepatic specific transcription factor, and metabolism-related cytochrome genes and integrin β1 (a regulator expressed during liver development) [39], suggests that BDPCs transdifferentiate or are hepatically programmed into hepatic epithelial cells. The transdifferentiation of $CD34^+$ cells into hepatocyte-like cells supports the theory of stem cell plasticity.

Therefore, we hypothesize that transplanted dBDPCs might act through two major mechanisms to promote liver regeneration after injury. One is by direct repopulation of the damaged tissue region by hepatic-differentiated donor cells. The other is that dBDPCs act indirectly by stimulating a regenerative repair response in local cells. In our animal liver injury model, transplanted GFP^+ dBDPCs repopulated the central vein region, where most pathological change occurs. This finding suggests that the in vitro expanded and differentiated BDPCs engraft into the recipient mouse liver and promote regeneration of the damaged tissue. Ki-67 is a marker that specifically represents cell proliferation during all active phases of the cell growth cycle but is absent from resting cells (G_0). Finding that Ki-67 and albumin are present in both GFP^+ cells and the adjacent liver cells suggests that the repopulated dBDPCs are proliferating and might secrete growth factors in the nearby regenerating liver tissue. Interestingly, less infiltration of inflammatory cells in the damaged regions and adjacent area was observed in dBDPC-treated animals, suggesting a possible immune inhibition or attenuation by dBDPCs. Considering that BDPCs have a high proliferation capacity and stem cell properties, we analyzed dBDPC-treated (and untreated) livers for tumor formation. We found no evidence of neoplasm formation in livers and all other organs at all time points up to our study limit of 3 months after dBDPC treatment. Although longer time course surveillance will be necessary in future studies, the most active influence of dBDPCs on liver regenerative repair likely occurs within the first weeks after treatment, with resolution of the liver injury.

CCl_4 is a potent hepatotoxic agent, and the natural recovery process for acute liver injury caused by CCl_4 peaks in over 1 week [40, 41]. To clearly distinguish between liver damage and transplanted cell regeneration, we increased the common dose from 0.8–1.0 ml/kg to 1.2 ml/kg CCl_4. The serum ALT levels increased to greater than 350 times normal by the enzyme release from the massive hepatocyte damage 24 hours after CCl_4 injection. In addition, 2 mice died (20% mortality) on days 2 and 3. Liver swelling and inflammation (hepatomegaly) on the day of sacrifice (day 7) and pathological alterations in the mouse livers occurs, demonstrating severe damage to the liver. However, livers from dBDPC-treated mice show a remarkable rescue, with amelioration of liver damage, regenerated liver structure, improved liver function, and greater overall animal survival.

Conclusion

In this study, BDPCs from adult mouse have been systematically identified and characterized. They can have rapid expansion and hepatic differentiation into functional hepatocyte-like cells in vitro. In the acute injury model, dBDPCs were injected intravenously through the retro-orbital sinus. Thus, dBDPCs first entered the peripheral circulation, where they were distributed systemically and able to traffic specifically to the injured liver. There, the transplanted GFP-positive dBDPCs engrafted in the necrotic area, proliferated, differentiated, and promoted regeneration of the mouse liver. Because of the ease of harvest, the ability to expand and differentiate in vitro, and the ease of intravenous delivery, dBDPCs have great potential as a cell-based therapy for liver diseases. Further experiments will assess the signal pathways that play key roles in expansion, differentiation, and transplantation of the BDPCs in mice and in humans, which will help to elucidate their functional role during liver regeneration and the mechanisms of interactions between dBDPCs and hepatic cells.

Acknowledgments

We thank Dr. Valentina Factor (NIH) for the kind donation of the A6 antibody, Dr. David Parks for help with FACS analysis, and Marty Bigos for his help with FACS sorting. We also thank Drs. Jill Helms and Karl Sylvester for advice and suggestions. This study was supported by research funding from the NIH (Grant R01 GM087609, to H.P.L.), a gift from Ingrid Lai and Bill Shu in honor of Anthony Shu (to H.P.L.), the Hagey Laboratory for Pediatric Regenerative Medicine, the American Society of Maxillofacial Surgeons/Maxillofacial Surgeons Foundation Research Grant Award (to H.P.L. and M.S.H.), and California Institute for Regenerative Medicine Clinical Fellow Training Grant TG2-01159 (to M.S.H.).

Author Contributions

M.H. and S.L.: conception and design, data analysis and interpretation, manuscript writing, final approval of manuscript; S.M.: identification and confirmation of mT/mG and albumin/Cre transgenes, data analysis and interpretation, manuscript editing, final approval of manuscript; B.L.: identification and confirmation of mT/mG and albumin/Cre transgenes, final approval of manuscript; M.S.H.: data analysis and interpretation, manuscript editing, final approval of manuscript; M.T.L.: manuscript editing, final approval of manuscript; H.P.L.: planning and coordination of the project, manuscript editing, final approval of manuscript.

Disclosure of Potential Conflicts of Interest

The authors indicated no potential conflicts of interest.

REFERENCES

1 Asrani SK, Larson JJ, Yawn B et al. Underestimation of liver-related mortality in the United States. Gastroenterology 2013;145:375–382.e1–2.

2 Schwartz RE, Fleming HE, Khetani SR et al. Pluripotent stem cell-derived hepatocyte-like cells. Biotechnol Adv 2014;32:504–513.

3 Forbes SJ, Alison MR. Regenerative medicine. Knocking on the door to successful hepatocyte transplantation. Nat Rev Gastroenterol Hepatol 2014;11:277–278.

4 Filippi C, Dhawan A. Current status of human hepatocyte transplantation and its potential for Wilson's disease. Ann N Y Acad Sci 2014; 1315:50–55.

5 Sokal EM. From hepatocytes to stem and progenitor cells for liver regenerative medicine: Advances and clinical perspectives. Cell Prolif 2011;44(suppl 1):39–43.

6 Kung JW, Forbes SJ. Stem cells and liver repair. Curr Opin Biotechnol 2009;20:568–574.

7 Alison MR, Islam S, Lim S. Stem cells in liver regeneration, fibrosis and cancer: The good, the bad and the ugly. J Pathol 2009;217:282–298.

8 Petersen BE, Bowen WC, Patrene KD et al. Bone marrow as a potential source of hepatic oval cells. Science 1999;284:1168–1170.

9 Fox IJ, Strom SC. To be or not to be: Generation of hepatocytes from cells outside the liver. Gastroenterology 2008;134:878–881.

10 Duncan AW, Dorrell C, Grompe M. Stem cells and liver regeneration. Gastroenterology 2009;137:466–481.

11 Nielsen JS, McNagny KM. Novel functions of the CD34 family. J Cell Sci 2008;121:3683–3692.

12 Sidney LE, Branch MJ, Dunphy SE et al. Concise review: Evidence for CD34 as a common marker for diverse progenitors. STEM CELLS 2014; 32:1380–1389.

13 Frändberg S, Boreström C, Li S et al. Exploring the heterogeneity of the hematopoietic stem and progenitor cell pool in cord blood: Simultaneous staining for side population, aldehyde dehydrogenase activity, and CD34 expression. Transfusion 2015;55:1283–1289.

14 Garg V, Garg H, Khan A et al. Granulocyte colony-stimulating factor mobilizes CD34(+) cells and improves survival of patients with acute-on-chronic liver failure. Gastroenterology 2012;142:505–512.e1.

15 Sharma M, Rao PN, Sasikala M et al. Autologous mobilized peripheral blood CD34(+) cell infusion in non-viral decompensated liver cirrhosis. World J Gastroenterol 2015;21:7264–7271.

16 Nakamura T, Torimura T, Iwamoto H et al. CD34(+) cell therapy is safe and effective in slowing the decline of hepatic reserve function in patients with decompensated liver cirrhosis. J Gastroenterol Hepatol 2014;29: 1830–1838.

17 Weissman I. Stem cell therapies could change medicine ... if they get the chance. Cell Stem Cell 2012;10:663–665.

18 Fox IJ, Daley GQ, Goldman SA et al. Stem cell therapy. Use of differentiated pluripotent stem cells as replacement therapy for treating disease. Science 2014;345:1247391.

19 Walasek MA, van Os R, de Haan G. Hematopoietic stem cell expansion: Challenges and opportunities. Ann N Y Acad Sci 2012;1266: 138–150.

20 Li S, Huang KJ, Wu JC et al. Peripheral blood-derived mesenchymal stem cells: Candidate cells responsible for healing critical-sized calvarial bone defects. STEM CELLS TRANSLATIONAL MEDICINE 2015;4:359–368.

21 Mossadegh-Keller N, Sarrazin S, Kandalla PK et al. M-CSF instructs myeloid lineage fate in single haematopoietic stem cells. Nature 2013; 497:239–243.

22 Okabayashi T, Shima Y, Sumiyoshi T et al. Extrahepatic stem cells mobilized from the bone marrow by the supplementation of branched-chain amino acids ameliorate liver regeneration in an animal model. J Gastroenterol Hepatol 2014;29:870–877.

23 Méndez-Ferrer S, Michurina TV, Ferraro F et al. Mesenchymal and haematopoietic stem cells form a unique bone marrow niche. Nature 2010;466:829–834.

24 Morrison SJ, Scadden DT. The bone marrow niche for haematopoietic stem cells. Nature 2014;505:327–334.

25 Doan PL, Chute JP. Ex vivo expansion of murine and human hematopoietic stem cells. Methods Mol Biol 2014;1185:211–221.

26 Muench MO, Beyer AI, Fomin ME et al. The adult livers of immunodeficient mice support human hematopoiesis: Evidence for a hepatic mast cell population that develops early in human ontogeny. PLoS One 2014;9:e97312.

27 Newsome PN. SOS liver damage: Calling all haematopoietic stem cells. Liver Int 2014; 34:1–3.

28 Soto-Gutiérrez A, Navarro-Alvarez N, Zhao D et al. Differentiation of mouse embryonic stem cells to hepatocyte-like cells by coculture with human liver nonparenchymal cell lines. Nat Protoc 2007;2:347–356.

29 Alaimo G, Cozzoli E, Marfe G et al. Blood-derived stem cells (BDSCs) plasticity: In vitro hepatic differentiation. J Cell Physiol 2013;228: 1249–1254.

30 Mu N, Liu HB, Meng QH et al. The differentiation of human multipotent adult progenitor cells into hepatocyte-like cells induced by coculture with human hepatocyte line L02. Ann Surg Treat Res 2015;88:1–7.

31 Wada W, Medina JJ, Kuwano H et al. Comparison of the function of the beta(C) and beta(E) subunits of activin in AML12 hepatocytes. Endocr J 2005;52:169–175.

32 Jelnes P, Santoni-Rugiu E, Rasmussen M et al. Remarkable heterogeneity displayed by oval cells in rat and mouse models of stem cell-mediated liver regeneration. Hepatology 2007;45:1462–1470.

33 Awuah PK, Nejak-Bowen KN, Monga SP. Role and regulation of PDGFRα signaling in liver development and regeneration. Am J Pathol 2013;182:1648–1658.

34 Dorrell C, Erker L, Lanxon-Cookson KM et al. Surface markers for the murine oval cell response. Hepatology 2008;48:1282–1291.

35 Van Arnam JS, Herzog E, Grove J et al. Engraftment of bone marrow-derived epithelial cells. Stem Cell Rev 2005;1:21–27.

36 Ullah M, Stich S, Notter M et al. Transdifferentiation of mesenchymal stem cells-derived adipogenic-differentiated cells into osteogenic- or chondrogenic-differentiated cells proceeds via dedifferentiation and have a correlation with cell cycle arresting and driving genes. Differentiation 2013;85:78–90.

37 Muzumdar MD, Tasic B, Miyamichi K et al. A global double-fluorescent Cre reporter mouse. Genesis 2007;45:593–605.

38 Snyder CS, Harrington AR, Kaushal S et al. A dual-color genetically engineered mouse model for multispectral imaging of the pancreatic microenvironment. Pancreas 2013;42:952–958.

39 Tanimizu N, Kikkawa Y, Mitaka T et al. α1- and α5-containing laminins regulate the development of bile ducts via β1 integrin signals. J Biol Chem 2012;287:28586–28597.

40 Weber LW, Boll M, Stampfl A. Hepatotoxicity and mechanism of action of haloalkanes: Carbon tetrachloride as a toxicological model. Crit Rev Toxicol 2003;33:105–136.

41 Zira A, Kostidis S, Theocharis S et al. 1H NMR-based metabonomics approach in a rat model of acute liver injury and regeneration induced by CCl4 administration. Toxicology 2013; 303:115–124.